The quantity Δ_h, which evaluates the net disruption of the solvent per solvating molecule, is related to the amount of hydrogen bonding in the solvent. It decreases with increasing temperature, as expected. It is the only quantity sensitive to secondary solvation effects. Since the nearest-neighbor interaction model suggests that Δ_h should be about 5 ppm for all ions, the observed values might be interpreted as representing some structure making near cations and some structure breaking near anions. This is quite speculative and contradicts the usual picture of secondary cation solvation.[30] There is no necessity that the degree of ordering correspond precisely to the proportion of hydrogen bonding.

All measured characteristics of the solvation process are essentially equal in water at +25° and methanol at −69°, that is, about 25° above the freezing point in each case. As a consequence of this, the molal shifts of cations in the two solvents are observed to be in the ratio of the solvent molecular weights.

Now that it is possible to evaluate separately the direct ion–molecule shift, the solvent shielding in ionic solutions may be used as a probe to evaluate more subtle effects of hydrogen bonding and liquid structure.

Acknowledgments. We wish to thank Mr. F. Fujiwara and Dr. B. Kratochvil for valuable discussions about some aspects of this work, and Jack Pannekoek and Mon Pon (our summer research assistants) for their help in the preparation of nearly 1000 nmr samples. This research was supported in part by National Research Council of Canada Grant No. A-2051.

Endor-Detected Nuclear Magnetic Resonance Studies of Small Ring Systems. I. $(CH_2)_3C(COOD)_2$[1a]

Larry R. Dalton[1b] and Alvin L. Kwiram*[1c]

Contribution from the Department of Chemistry, Harvard University, Cambridge, Massachusetts 02138.
Received March 2, 1972

Abstract: A technique for observing enhanced proton and deuteron magnetic resonance in single crystals of $(CH_2)_3C(COOD)_2$ is described. From an investigation of the proton dipolar and deuteron quadrupolar interactions, the conformation of the $(CH_2)_3C(COOD)_2$ molecules and the relationship of the molecules to the external morphology of the crystal are established. Molecules of 1,1-cyclobutanedicarboxylic acid at 4.2°K were found to be bound together by hydrogen-bonded carboxylic acid bridges which zigzag along the crystallographic *c* axis. The normal to the plane of the slightly puckered four-membered ring also lies approximately along the *c* axis with the C–C bonds of the ring oriented approximately along the *a* and *b* axes. The spatial separation between geminal protons is found to be 1.895 Å. The proton ednmr data are best described by a dihedral angle of 165°, a C–H distance of 1.10 Å, and an H–C–H angle of 116°.

It has been known for some time that structural information can be gained by investigating the nuclear magnetic resonance (nmr) of oriented single crystals;[2–9] however, studies involving the conventional wide-line nmr technique are often fraught with difficulties. Sensitivity is a serious problem particularly for nuclei with small magnetic moments or those present in low concentration. Moreover, radiofrequency saturation is a problem particularly at low temperatures (less than 10°K) but often even at ambient temperatures. The investigation of malonic acid by Derbyshire, *et al.*,[9] provides an example of the difficulty of applying the wide-line nmr technique to the study of organic single crystals. Even at ambient temperatures, 5-hr scans were required to avoid saturating the deuteron magnetic resonance of perdeuteriomalonic acid crystals. Minor over-modulation and radiofrequency saturation resulting in some line-shape distortion were necessary to produce signals above the noise level.

Hahn and coworkers[10–17] have developed a pulsed multiple resonance technique for significantly enhancing the resonance signals of nuclei present in small concentrations by monitoring changes in the resonance signal of a more abundant species of nuclei. Inherent to the success of such experiments is the criterion that two species of nuclei be effectively coupled by nuclear spin diffusion and that this spin diffusion be fast relative to spin–lattice relaxation times. The technique of Hahn and coworkers has proved to be eminently successful; the following species have been detected in natural abundance: ^{41}K (7%), ^{40}K (0.012%), ^{43}Ca (0.13%), ^{13}C (1.1%), and ^{2}H (0.016%).

---

(1) (a) This work was supported by National Science Foundation Grants GP-4612 and GP-7428. (b) National Institutes of Health Predoctoral Fellow, 1966–1970; (c) Alfred P. Sloan Fellow; author to whom correspondence should be addressed at Department of Chemistry, University of Washington, Seattle, Wash. 98105.

(2) (a) G. E. Pake, *J. Chem. Phys.*, **16**, 327 (1948); (b) S. Ketudat and R. V. Pound, *ibid.*, **26**, 708 (1957).

(3) T. Chiba, *ibid.*, **39**, 947 (1963).

(4) T. Chiba, *ibid.*, 41, 1352 (1964).

(5) B. Pedersen, *Acta Crystallogr.*, 20, 412 (1966).

(6) M. Weissman, *J. Chem. Phys.*, 44, 422 (1966).

(7) R. Blinc and D. Hadzi, *Nature (London)*, 212, 1307 (1966).

(8) B. Pedersen, *Acta Chem. Scand.*, 22, 453 (1968).

(9) W. Derbyshire, T. C. Gorvin, and D. Warner, *Mol. Phys.*, 17, 401 (1969).

(10) S. R. Hartmann and E. L. Hahn, *Phys. Rev.*, 128, 2042 (1962).

(11) R. E. Slusher and E. L. Hahn, *Phys. Rev. Lett.*, 12, 246 (1964); *Phys. Rev.*, **166**, 332 (1968).

(12) E. L. Hahn, *Proc. Colloq. AMPERE*, **13**, 42 (1964).

(13) C. J. Gabriel, Thesis, University of California, Berkeley, 1964.

(14) D. McArthur, Thesis, University of California, Berkeley, 1967.

(15) M. Schwab, Thesis, University of California, Berkeley, 1968.

(16) M. Schwab and E. L. Hahn, *J. Chem. Phys.*, **52**, 3152 (1970).

(17) E. P. Jones and S. R. Hartmann, *Phys. Rev. Lett.*, **22**, 867 (1969).

Another technique capable of producing substantial enhancement of nuclear magnetic resonance (nmr) signals is that of endor detection of nmr (ednmr).[18] The distant endor effect, on which this technique is based, was first observed by Lambe and coworkers[19,20] and has been exploited by Kwiram and coworkers[18,21–23] to study molecular structure and dynamics. The ednmr experiment is schematically represented in Figure 1 and has the following characteristics. A small concentration of paramagnetic centers is introduced into the crystal by doping or exposure to high energy radiation.[24] The application of an intense (saturating) microwave field at the resonance frequency of the unpaired electrons results in a polarization of the local or weakly coupled[25] nuclei with a corresponding enhancement of nuclear resonance signals by factors of 10^2 to 10^3. The polarization of the local nuclei is transmitted to the distant[25] nuclei by the action of nuclear spin diffusion (nuclear spin flip–flop transitions). If the nuclear resonance of the distant nuclei is excited by a radiofrequency field, the steady-state nuclear polarization will be disturbed, and this perturbation is *detected* by monitoring the transient change in absorption of microwave energy by the electron spin system. In other words the electrons perform two functions: (1) enhancement of nuclear polarization and (2) detection of nuclear resonance.

A detailed treatment of the spin kinetics involved in the ednmr experiment is a formidable undertaking. For example, there exist three possible mechanisms by which the steady-state nuclear polarization can be effected. The first mechanism is the well-known "solid effect" in which the microwave field flips simultaneously one electron and one nuclear spin.[26] The other mechanisms are two-step effects which may be described as dynamic polarization by cooling of the electron interactions. As a result of the existence of electron dipole–dipole interactions, the intense microwave field can effect a cooling of electron interactions (the electron Zeeman and spin–spin reservoirs will exhibit different spin temperatures and spin–lattice relaxation times).[27,28] In the first of the two-step processes, this cooling is transmitted to the nuclear spins by the double transitions of the solid effect.[29] In the second two-step process, the cooling of the electron interactions is transmitted to the nuclear spins by three-spin processes in which, simultaneously, two electron spins exchange their spin orientation and a nuclear spin flips.[30] The two-step processes are probably the most important in the systems discussed here.[18,31]

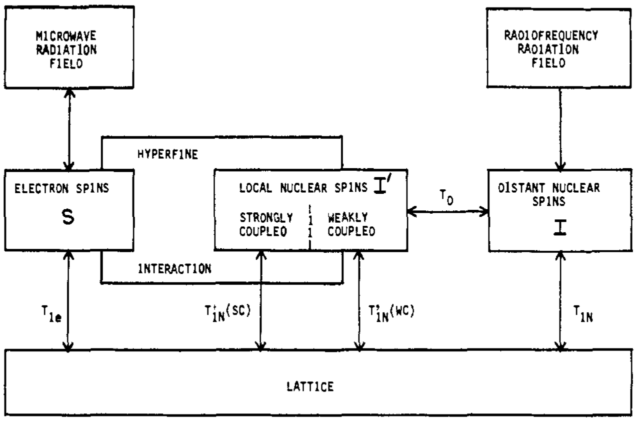

Figure 1. A schematic diagram of the energy transfer processes involved in the ednmr experiment is shown. T_{1e} is the electron spin-lattice relaxation time (in the presence of an intense microwave field, the electron Zeeman and dipolar reservoirs exhibit different spin temperatures and spin–lattice relaxation times), T_{1N} is the nuclear spin-lattice relaxation time (in the presence of effective cross relaxation the weakly coupled and strongly coupled nuclei will exhibit the same spin-lattice relaxation time), and T_D is the nuclear spin diffusion time.

The process of transfer of nuclear spin polarization from the local (strongly and weakly coupled nuclei) to the distant nuclei depends strongly upon molecular and crystal symmetry and the distribution of hyperfine interactions present in the pool of local nuclei. As a result of the requirement of energy conservation, the most efficient transfer is expected for the case of near-zero hyperfine interactions in the local pool. However, if the electrons are strongly coupled by dipolar or cross relaxation, then even strongly coupled nuclei may contribute indirectly to distant nuclear polarization through the weakly coupled proton pool.

The polarization of rare nuclear species (*e.g.*, ^{13}C, ^2H, and ^{17}O) will be affected by the transport of polarization among different species of distant nuclei. The requirement of energy conservation is most important in determining the effectiveness of spin exchange among the distant nuclei. As a result of this requirement one might anticipate observing stronger natural abundance ^{13}C signals in a deuterium enriched hydrocarbon system than would be observed for the protonated system. Indeed such effects have been observed.[22,23]

In the preceding paragraphs we have presented a qualitative description of the fundamentals of the ednmr experiment; a more quantitative treatment must await a more exacting study of the spin kinetics. In the dis-

---

(18) R. C. McCalley and A. L. Kwiram, *Phys. Rev. Lett.*, **24**, 1279 (1970).

(19) R. W. Terhune, J. Lambe, G. Makhov, and L. G. Cross, *ibid.*, **4**, 234 (1960).

(20) J. Lambe, N. Laurance, E. C. McIrvine, and R. W. Terhune, *Phys. Rev.*, **122**, 1161 (1961).

(21) L. R. Dalton and A. L. Kwiram, *Bull. Amer. Phys. Soc.*, **16**, 93 (1971).

(22) R. C. McCalley, Thesis, Harvard University, Cambridge, 1971.

(23) L. R. Dalton, Thesis, Harvard University, Cambridge, 1971.

(24) In practice the requirement of a small concentration of paramagnetic contaminants can frequently be quite easily achieved. We have conducted preliminary studies on 2,2,5,5-tetramethylpyrrolidine-3-carboxamide and 2,2,5,5-tetramethylpyrrolidine-3-carboxylic acid doped with 2,2,5,5-tetramethylpyrrolidine-3-carboxamide-1-oxyl, X-irradiated crystals of urea doped with organic acids, and X-irradiated organic dicarboxylic and amino acids. As the concentration of radicals needed for a successful ednmr experiment is of the order of one part in 10,000, the structure of the host is not significantly perturbed by the introduction of the paramagnets.

(25) Local nuclei are defined as those nuclei which experience finite hyperfine interaction with the paramagnetic electron of the damage center or impurity while distant nuclei experience no hyperfine interaction with the paramagnetic electrons. A range of hyperfine interaction energies will in general be associated with the local nuclear pool and these are arbitrarily separated into strongly coupled (>5 MHz) and weakly coupled (<5 MHz) interactions. Since these are tightly coupled by electron cross relaxation at low temperatures, we can characterize the local pool by a single spin temperature and spin–lattice relaxation time. The nuclear spin energy levels of the distant nuclei are unperturbed by the introduction of the paramagnetic electrons.

(26) A. Abragam and W. G. Proctor, *C. R. Acad. Sci.*, **246**, 2253 (1958).

(27) A. G. Redfield, *Phys. Rev.*, **98**, 1787 (1955).

(28) B. N. Provotorov, *Zh. Eksp. Teor. Fiz.*, **41**, 1582 (1961); *Sov. Phys. JETP*, **14**, 1126 (1962).

(29) A. Abragam and M. Borghini, *Progr. Low Temp. Phys.*, **4**, 384 (1964).

(30) M. Borghini, *Phys. Lett. A*, **26**, 242 (1968).

(31) W. Th. Wenckebach, L. A. H. Schreurs, H. Hoogstraate, T. J. B. Swanenburg, and N. J. Poulis, *Physica*, **52**, 455 (1971).

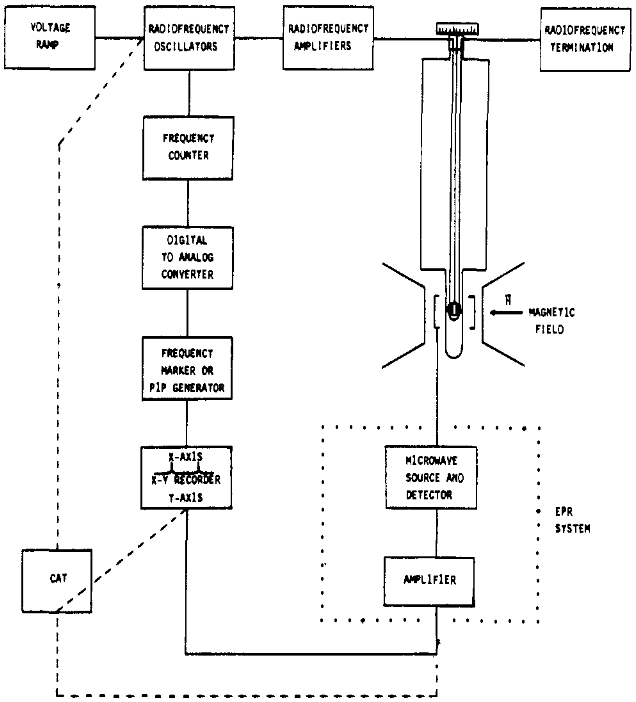

Figure 2. A schematic diagram of the endor apparatus is shown. The dashed lines indicate an alternate arrangement in which a computer of average transients (CAT) is used to ramp the radiofrequency oscillators and detect the ednmr signals.

cussion that follows we shall demonstrate the observation of enhanced proton and deuteron magnetic resonance in single crystals of 1,1-cyclobutanedicarboxylic acid (1,1-CBDA). A method for determining the conformation of the molecules in the unit cell from magnetic resonance data is described. The results of this study are compared with the results of a recent X-ray crystallographic determination of the structure of 1,1-CBDA by Soltzberg and Margulis.[32]

The present communication demonstrates the utility of the ednmr technique for the analysis of molecular structure and dynamics. As the nuclear dipolar and quadrupolar interactions determined from ednmr measurements are extremely sensitive to the relative positions of nuclei and the relative motion of nuclei, ednmr affords a microscopic probe of structure which is highly complementary to the neutron diffraction technique and the X-ray crystallographic technique for locating the relative positions of light atoms such as protons. As ednmr measurements can be conveniently carried out at temperatures as low as 1.2°K and at variable temperatures over the range 1.2 to 20°K the technique is particularly suited for the study of molecular motion.

Experimental Section

Preparation of Samples. 1,1-CBDA purchased from Aldrich Chemical Co. was treated with decolorizing carbon (Norit) and recrystallized from water three times. Deuteration of 1,1-CBDA in the carboxylic acid position was effected by exchange with D_2O. Ten grams (0.08 mol) of the recrystallized acid was dissolved in 40 g of D_2O (Bio-Rad, 99.9%; 2 mol), the solution was heated to 60°, and then the solvent was evaporated at reduced pressure. Four additional exchanges with D_2O were carried out, the progress of the deuteration being monitored by the increase in intensity of the COOD infrared band relative to the COOH absorption. Single crystals of $(CH_2)_3(COOD)_2$ were obtained by slow evaporation of a D_2O solution in a vacuum desiccator.

Instrumentation. A schematic representation of the two instrumental arrangements employed is shown in Figure 2. Operation of this equipment has been described elsewhere[33] and will be reviewed only briefly here.

All data reported in this communication were recorded on crystals X-irradiated from 1 to 15 min at ambient temperatures and cooled to 4.2°K. The radiofrequency oscillators indicated in Figure 2 were swept by applying the output of a homemade voltage ramp or the output of a computer-of-averaged-transients to the oscillators. Frequency markers were placed on the spectra at 10-kHz intervals. Data were recorded at a maximum scale expansion of 10 kHz/in. and a minimum sweep rate of 10 kHz/min.

Data Collection. By standard X-ray techniques single crystals of 1,1-CBDA were found to be monoclinic with space group $P2_1/c$. Relevant crystal data can be summarized as follows:[34] $a = 6.12 \pm 0.01$ Å, $b = 10.52 \pm 0.05$ Å, $c = 11.01 \pm 0.02$ Å; $\beta = 99.64 \pm 0.10°$; $Z = 4$; and $\rho = 1.36$ g/cc. These values can be compared with the more precise data of Soltzberg and Margulis.[32]

Crystals of 1,1-CBDA grow as rectangular prisms usually somewhat elongated along the *a* axis. The *ac* plane is a well-defined cleavage plane. The ednmr data to be discussed were taken by rotating the $a, b, c^* = a \times b$ crystal axis system with respect to a fixed external magnetic field. Crystals were mounted on the rotatable sample holder with the aid of optical goniometry. This procedure permitted crystal alignment relative to the upper control dial of the sample rotator with an error of the order of 0.25°.

In order to obtain accurate and convenient alignment of the crystals employing optical goniometry, crystals of approximately 5 × 2 × 2 mm were employed. Certainly substantially larger or smaller crystals could have been used.

Deuteron and proton dipolar tensors were determined by recording ednmr spectra at 2 to 5° intervals for rotations through at least 180° in the *ab*, *ac**, and *bc** planes. A different crystal of $(CH_2)_3C(COOD)_2$ was employed for each plane of rotation, and each plane of rotation was investigated twice for the purpose of obtaining precise ednmr tensors. Some ednmr data were recorded in the *bc* plane and in the skew plane obtained using the bisector of the *ac** plane as an axis of sample rotation. These supplemental data were taken solely for the purpose of correctly matching lines from the four molecules per unit cell at the intersections of the *ab*, *ac**, and *bc** planes. (Because of the twofold symmetry involved, magnetic resonance lines arising from the same interaction in the four different molecules per unit cell coalesce when the field is oriented along the *b* axis or is in the *ac* plane.)

Data Analysis: Deuteron Quadrupole Tensors. The quadrupole interaction for the carboxylic acid deuterons of $(CH_2)_3C(COOD)_2$ is described by the Hamiltonian[35]

$$H_Q = \frac{e^2qQ}{4I(2I-1)}[3I_z^2 - I(I+1) + \frac{1}{2}\eta(I_+^2 + I_-^2)] \quad (1)$$

where $eq = V_{zz}$ and $\eta = (V_{xx} - V_{yy})/V_{zz}$. V_{zz} is the principal element of the quadrupole tensor and η is the asymmetry parameter defined to be positive.

In the high-field limit, where the nuclear Zeeman energy $\mathcal{H}_{NZ} = -g_n\beta_n\mathbf{I}\cdot\mathbf{H}$ is much larger than the quadrupole energy, the splitting between the two $\Delta M_I = \pm 1$ quadrupole transitions of the deuteron is given by first-order perturbation theory as

$$\Delta\nu = (3/4)(e^2qQ/h)[(3\cos^2\theta - 1) + \eta\sin^2\theta\cos 2\phi] \quad (2)$$

where θ and ϕ are the spherical polar angles relating the magnetic field direction to the principal axes of the quadrupole tensor.

The deuteron ednmr data obtained for rotation in the three orthogonal planes *ab*, *ac**, and *bc** were obtained by performing a least-squares fitting of the splitting between the $\Delta M_I = \pm 1$ lines to the following expressions.

---

[32] L. Soltzberg and T. N. Margulis, *J. Chem. Phys.*, **55**, 4907 (1971).

[33] A. L. Kwiram, *ibid.*, **55**, 2484 (1971).

[34] The assistance of Dr. John Wormald is greatly appreciated.

[35] A. Abragam, "The Principles of Nuclear Magnetism," Clarendon Press, Oxford, 1962, Chapter VII.

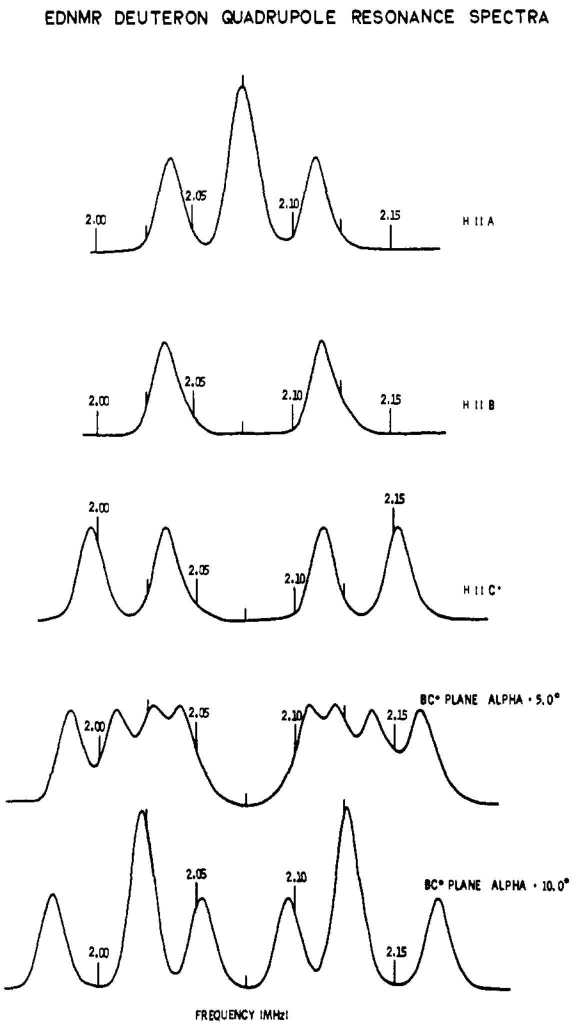

Figure 3. Typical deuteron magnetic resonance spectra of single crystals of $(CH_2)_3C(COOD)_2$ obtained employing the ednmr technique are shown. α defines the angle between the dc magnetic field and the c^* axis.

$$\begin{aligned}\Delta\nu_{ab} &= V_{aa}\cos^2\beta + 2V_{ab}\cos\beta\sin\beta + V_{bb}\sin^2\beta\\ \Delta\nu_{ac^*} &= V_{aa}\sin^2\alpha + 2V_{ac^*}\cos\alpha\sin\alpha + V_{c^*c^*}\cos^2\alpha \qquad (3)\\ \Delta\nu_{bc^*} &= V_{bb}\sin^2\alpha + 2V_{bc^*}\cos\alpha\sin\alpha + V_{c^*c^*}\cos^2\alpha\end{aligned}$$

where α and β are the spherical polar angles relating the magnetic field to the abc^* axis system. The principal elements of the quadrupole tensors and the direction cosines relating these elements to the a, b, and c^* axes are obtained by diagonalizing the 3 × 3 matrix.

$$\begin{vmatrix} V_{aa} & V_{ab} & V_{ac^*} \\ V_{ab} & V_{bb} & V_{bc^*} \\ V_{ac^*} & V_{bc^*} & V_{c^*c^*} \end{vmatrix}$$

Data Analysis: Proton Dipole Tensors. The dipolar Hamiltonian describing the interaction between two proton magnetic moments can be written as[36]

$$H_D = g_p{}^2\beta_n{}^2\left\{\frac{\mathbf{I}_i\cdot\mathbf{I}_j}{r^3} - \frac{3(\mathbf{I}_i\cdot\mathbf{r})(\mathbf{I}_j\cdot\mathbf{r})}{r^5}\right\} \qquad (4)$$

The splitting between the two $\Delta M_I = \pm 1$ transitions in the high field limit is given by

$$\Delta\nu = (3/2)g_p{}^2\beta_n{}^2(1 - 3\cos^2\theta)/r^3 = D(1 - 3\cos^2\theta) \qquad (5)$$

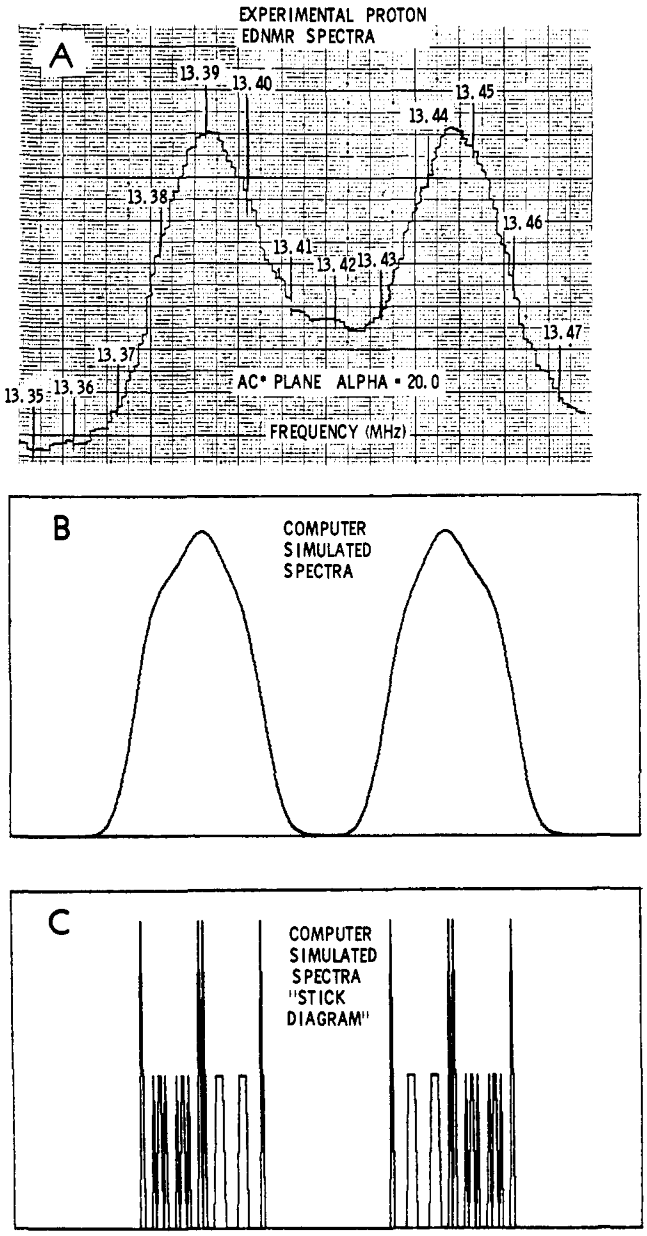

Figure 4. (A) A typical proton magnetic resonance spectrum of $(CH_2)_3C(COOD)_2$ obtained employing the ednmr technique is shown. The spectrum was obtained with the dc magnetic field oriented in the ac^* plane 20° from the c^* axis. The 1-KHz steps evident in this figure simply reflect the resolution of the digital-to-analog converter. (B) The computer simulated proton magnetic resonance spectrum calculated for this orientation assuming that the hydrocarbon ring exists in a single statically puckered conformation with a dihedral angle of 164.5°, no methylene rocking, C–H distance = 1.095 Å, and ∠HCH = 116°. (C) A computed "stick" diagram for the geminal, vicinal, and transannular proton dipolar splittings of the above model (4B) is given.

where θ is the polar angle relating the magnetic field **H** to the principal axis of the dipolar tensor. D and the direction cosines relating the dipole–dipole interaction direction to the a, b, c^* axes were evaluated by performing a least-squares analysis of the dipole–dipole splitting measured in the ab, ac^*, and bc^* planes.

Results and Interpretation

The ednmr signal characteristics observed for the $(CH_2)_3C(COOD)_2$ system are quite similar to those observed for other systems.[18,22] An enhancement of the nuclear resonance signal by a factor of 10^2 to 10^3 is observed and the signal response time (the time re-

---

(36) Reference 35, Chapter IV.

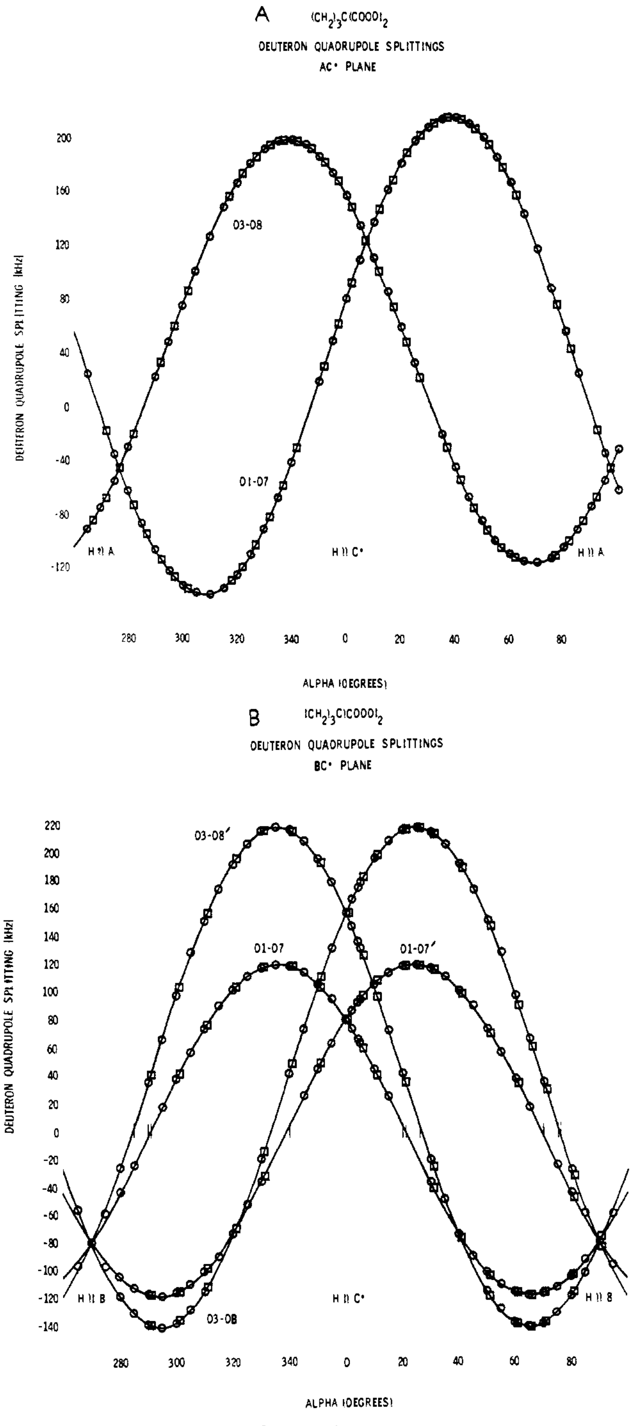

Figure 5. Typical plots of the splitting between the $\Delta M_I = \pm 1$ deuteron quadrupole resonance lines as a function of orientation of the dc magnetic field with respect to the *a*, *b*, and c^* axes are shown. Alpha is the angle between the dc field and the c^* axis. (A) illustrates the behavior of the splittings for rotation of the field in the ac^* plane. The circles and squares indicate data taken on different crystals on different dates. (B) demonstrates the variation of the splitting for rotation of the field in the bc^* plane.

quired for steady-state polarization to be reestablished after passage of the radiofrequency field through resonance) is of the order of a few seconds at 4.2°K. This latter feature makes the introduction of computer averaging techniques most convenient and such techniques were employed to enhance the natural abundance ^{13}C spectra. The strong signal to noise ratios observed for the deuteron and proton resonance signals made direct analysis of single scan spectra most practical.

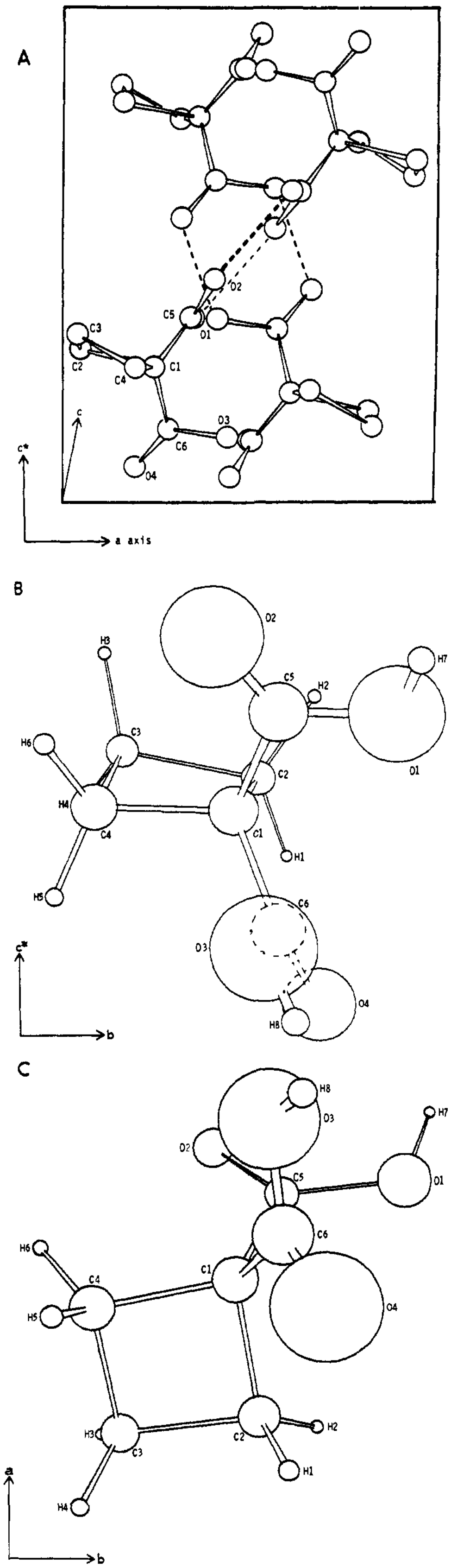

Figure 6. Perspective drawings of the conformation of 1,1-CBDA giving the best fit of the ednmr data are shown. Portion A illustrates the positioning of the four molecules in a unit cell (only the relative positioning of molecules can be fixed employing ednmr data). The cell is viewed along the *b* axis. Protons are omitted for the sake of clarity. (B) and (C) show one of the molecules per unit cell viewed along the *a* and *c* axes, respectively.

Table I. Deuteron Quadrupole and Proton Dipolar Tensors Determined for $(CH_2)_3C(COOD)_2$ Using the Ednmr Technique

Deuteron Tensors								
Deuteron	Tensor[a]			Eigenvalues[a]	Eigenvectors			
O1–D7	-5.599	∓ 62.114	-172.363	$V_{zz} = 251.835 \pm 1.5$	a	$(-0.582$	0.738	$-0.369)$
	∓ 62.114	-79.473	± 88.423	$V_{yy} = -139.649 \pm 1.5$	b	$(\pm 0.311$	∓ 0.186	$\mp 0.924)$
	-172.363	± 88.423	79.885	$V_{xx} = -112.186 \pm 1.5$	c^*	$(0.751$	0.649	$0.101)$
	Quadrupole coupling[a] Constant, $e^2qQ/h = 167.89 \pm 1.5$			Asymmetry parameter $\eta = 0.109 \pm 0.006$				
O3–D8	-74.423	∓ 58.576	106.841	$V_{zz} = 261.087 \pm 1.5$	a	$(0.340$	0.292	$-0.896)$
	∓ 58.576	-79.926	∓ 135.372	$V_{yy} = -144.798 \pm 1.5$	b	$(\mp 0.395$	± 0.907	$\pm 0.138)$
	106.841	∓ 135.833	156.101	$V_{xx} = -116.288 \pm 1.5$	c^*	$(0.853$	0.303	$0.423)$
	$e_sqQ/h = 174.06 \pm 1.5$				$\eta = 0.109 \pm 0.006$			

Proton Tensors								
		D(geminal)[a]			D(vicinal–estimated)[a]			
		β(H1–H2)	β(H3–H4)	β(H5–H6)	β(H1–H4)	β(H2–H3)	β(H5–H4)	β(H6–H3)
		28.0 ± 0.5	28.0 ± 0.5	28.0 ± 0.5	14.0 ± 2.0	14.0 ± 2.0	14.0 ± 2.0	14.0 ± 2.0
Direction	a	-0.258	-0.436	-0.403	0.177	0.035	0.886	0.860
cosines	b	± 0.158	± 0.124	∓ 0.064	∓ 0.952	∓ 0.979	± 0.128	± 0.277
	c^*	0.953	0.891	0.913	0.249	0.199	0.445	0.428

[a] All tensor elements and eigenvalues are in kHz. The spectral resolution was not sufficient to permit direct measurement of the vicinal proton dipolar splittings. The above values were obtained from computer simulation of the experimental spectra.

Typical deuteron and proton ednmr spectra are shown in Figures 3 and 4. Splitting of the ^{13}C nuclear resonance line due to ^{13}C–H dipolar interaction was unresolvable so all structural information had to be derived from a consideration of deuteron quadrupolar and proton dipolar interactions. Plots of the deuteron quadrupolar splitting between the $\Delta M_I = \pm 1$ transitions are shown in Figure 5. In Table I we summarize the information obtained concerning the quadrupolar and dipolar interactions in the $(CH_2)_3C(COOD)_2$ molecule. By employing the data in Table I, the conformation of the four molecules per unit cell can be related to the crystal morphology.

Qualitatively the procedure for relating ednmr data to molecular structure can be described as follows. To the electric field gradient (efg), q, at a deuteron site, there is a positive contribution from the various discrete nuclei nearby, and a negative (and smaller) contribution from the diffuse electron clouds, resulting in a net positive field gradient at the deuteron site.[4] The 1s electron on the deuteron contributes nothing to the efg, so that the principal field gradient axis (Z) is essentially parallel to the D–O bond direction, and the axis of the most negative efg element (Y) is roughly normal to the plane determined by the nuclei bonded to O. Thus to fix the conformation of the carboxylic acid bridge planes with respect to the crystallographic axes (or the a, b, and c^* axes) we assume that the O—D···O direction corresponds to the direction cosines of the V_{zz} element while the direction cosines of the V_{yy} element are assumed to define the normal to the carboxylic acid bridge plane.

As is evident from eq 5 the spatial separation of two interacting protons can be simply calculated from the experimentally determined D values. The direction cosines of the principal element of the dipolar tensor describes the direction of a vector connecting the interacting protons. From a complete analysis of the geminal, vicinal, and transannular dipolar interactions, the structure and conformation of the four-membered hydrocarbon ring can be determined. The geminal interactions are quite well resolved and the tensors describing these interactions were obtained from a least squares analysis of the dipolar splittings in orthogonal planes as described in the Experimental Section. Unfortunately spectral resolution was not sufficient to permit a direct analysis of the vicinal and transannular interactions. Consequently these tensors were obtained from computer simulation of the experimental spectra in the following manner. Structures and relative orientations for the four molecules per unit cell were assumed and proton ednmr spectra for the ab, ac^*, and bc^* planes were computed for these hypothetical structures employing eq 5. The restrictions placed on the choice of conformations were that the separation between geminal protons be 1.859 Å, consistent with the analysis of the geminal splittings, and that the directions of vectors connecting the geminal protons are those given in Table I. The conformation of the carboxylic acid bridge planes were assumed to be defined by the deuteron quadrupole tensor elements as previously described.

Initial calculations of spectra were carried out utilizing the following structural assumptions.

(1) The C–C–C angles of the four-membered ring are assumed to equal 90°.

(2) The following bond distances (Å) were assumed: C—C (endocyclic), 1.55; C—C (exocyclic), 1.50; C=O, 1.23; C—O, 1.30; O—H, 1.00; O···H, 1.60.

(3) The hydrocarbon ring was assumed to be puckered with a dihedral angle of 165° and with no methylene rocking. A C–H distance of 1.095 Å and an H–C–H angle of 116° were assumed.

Numerous spectra were computed for models with various values of the dihedral angle, the angle describing the methylene rocking, C–H distance, H–C–H angle, and C–C distance. Spectra were computed assuming the existence of both symmetrical (for which a pseudo-twofold rotation about an axis bisecting the C_β–C_α–C_β angle exists—both puckered forms are present) and asymmetrical barriers to ring inversion (for which the pseudo-twofold rotation does not exist—only one form is present).

Computer perspective drawings of the model resulting in the best reproduction of the experimental spectra are shown in Figure 6. It must be noted that dihedral angles of 166, 167, and 168° with 1, 2, and 3° of methylene rocking, respectively, would also describe the data nearly as well as the best fit model; moreover, slightly longer C–H bond distances and slightly smaller H–C–H angles may also be employed without significantly worsening the fit to the experiment data although a noticeable deterioration in the fit is apparent for the extreme values of C–H = 1.139 Å and an H–C–H angle of 109.5°. The 4.2°K ednmr data support the existence of only one statically puckered conformation, indicating that ring puckering in 1,1-CBDA must be described by an asymmetric double well potential.

Discussion

Correlation of the Structure of the Host Molecules with the Structure of the Cyclobutyl-1-carboxylic Acid Radical. While investigating the enhanced nuclear resonance of the host 1,1-CBDA molecules by ednmr we also recorded and analyzed the endor spectra of the cyclobutyl-1-carboxylic acid radical formed by X-irradiation. The endor spectra recorded at 4.2°K indicate that the four-membered ring of the radical exists in a static pucker (or, more correctly, is inverting at a rate much less than the hyperfine splitting difference of the β axial and equatorial protons) while the endor spectra at 77°K indicate that at this temperature the hydrocarbon ring is inverting rapidly (at a rate much greater than the hyperfine difference frequency). These observations are consistent with pulsed microwave measurements of the electron spin–lattice relaxation time of the radical over the temperature range 1–300°K.[37] Relaxation measurements indicate a low barrier to ring inversion and a separation between the ground and first excited vibrational state of 9.0 cm^{-1}.

For the purpose of correlation of the structures of the radical and host molecules we reproduce the hyperfine tensors for the protons of the radical ring determined from the 4.2°K endor data. From the tensors given in Table II it is clear that the puckering of the ring of the radical is described by an asymmetrical barrier, as only one puckered form is observed. From Table II it is also evident that the hydrocarbon ring of the radical is not symmetric with respect to the plane containing the bisector of the C_β–C_α–C_β angle and orthogonal to the C_β–C_α–C_β plane. This could be attributed to a skew puckering of the hydrocarbon ring or an unsymmetrical distribution of the unpaired electron density with respect to the aforementioned plane. Both effects could be attributed to the presence of the remaining carboxylic acid group.

Table II. β and γ Hyperfine Tensors for the Cyclobutyl-1-carboxylic Acid Radical in X-Irradiated 1,1-Cyclobutanedicarboxylic Acid

Proton	Fermi element, MHz	Eigen-values, MHz	Direction cosines *a*	*b*	*c**
Axial		118.22	0.787	±0.617	0.023
β	110.91	107.50	−0.259	∓0.343	0.903
Large		107.01	0.595	∓0.755	0.277
Axial		112.15	−0.542	∓0.681	0.493
β	104.50	101.01	−0.134	±0.507	0.851
Small		100.34	0.812	∓0.578	0.087
Equatorial		77.32	0.972	±0.147	−0.181
β	69.29	66.07	−0.144	∓0.235	−0.961
Large		64.48	0.182	∓0.964	−0.194
Equatorial		65.61	0.751	∓0.606	−0.262
β	57.08	53.42	−0.635	∓0.772	−0.028
Small[a]		52.21	−0.242	±0.117	−0.963
Axial		15.93	0.673	∓0.728	0.132
γ	11.33	9.81	−0.604	∓0.436	0.667
		8.25	0.430	±0.530	0.730
Equatorial		12.41	0.794	∓0.604	0.072
γ	7.76	6.49	0.582	±0.788	−0.198
		4.38	−0.181	∓0.123	0.976

[a] Because of spectral overlap the root-mean-square error for the equatorial β small interation is approximately 0.1 MHz compared to 0.04–0.01 MHz for the other protons.

It may be noted that the general relationship of the position of the hydrocarbon ring of the radical to that of the host molecules should depend strongly on the hybridization of the α carbon in the radical. We can quite reasonably anticipate that the hydrogen bonding of the remaining carboxylic acid group is largely undisturbed by the formation of the radical. If the α carbon is sp^2 hybridized, it is reasonable to expect the ring of the radical to be rotated through an angle of 55° from the position in the undamaged molecules as this new position would afford minimum steric interaction with the remaining carboxyl group. However, because of steric interactions with neighboring molecules, such a rotation is unlikely. If sp^3 hybridization of the α carbon is retained in the radical, the spatial reorientation of the ring should be significantly less. In Table III we compare the direction cosines of the principal elements of the dipolar tensors in the radical with the direction cosines of vectors pointing from C_α

Table III. Comparison between the Direction Cosines of the Electron-Nuclear Dipolar Hyperfine Elements in the Cyclobutyl-1-carboxylic Acid Radical and the Direction Cosines of the C_α–$H_{(\beta,\gamma)}$ Vectors of the Host Molecules

		Experimental dipolar elements			C_α–$H_{(\beta,\gamma)}$ vectors
		Axial β Large			
		7.31	−3.90	−3.41[a]	
Direction cosines	*a*	0.787	0.595	−0.259	0.721
	b	0.617	−0.755	−0.343	0.395
	*c**	0.023	0.277	0.903	0.569
		Equatorial β Large			
		8.03	−4.81	−3.22	
Direction cosines	*a*	0.972	0.182	−0.144	0.937
	b	0.147	−0.964	−0.235	0.263
	*c**	−0.181	−0.194	−0.961	−0.230
		Axial β Small			
		7.65	−4.16	−3.49	
Direction cosines	*a*	−0.542	0.812	−0.134	−0.153
	b	−0.681	−0.578	0.507	−0.933
	*c**	0.493	0.087	0.851	0.326
		Equatorial β Small			
		8.53	−4.87	−3.66	
Direction cosines	*a*	0.751	−0.242	−0.635	0.185
	b	−0.606	0.117	−0.772	−0.880
	*c**	−0.262	−0.963	−0.028	−0.438
		Axial γ			
		4.60	−3.08	−1.52	
Direction cosines	*a*	0.673	0.430	−0.604	0.601
	b	−0.728	0.530	−0.436	−0.507
	*c**	0.132	0.731	0.667	0.618
		Equatorial γ			
		4.65	−3.38	−1.27	
Direction cosines	*a*	0.794	−0.181	0.582	0.834
	b	−0.604	−0.123	0.788	−0.552
	*c**	0.072	0.976	−0.198	0.025

[a] All diagonal elements are in MHz.

---

(37) L. R. Dalton, A. L. Kwiram, and J. A. Cowen, Abstracts, Third Southeastern Magnetic Resonance Conference, Oak Ridge, Tenn., Oct 1971, No. C3; L. R. Dalton, A. L. Kwiram, and J. A. Cowen, submitted for publication.

Table IV. β Hyperfine Interactions in Alicyclic Radicals

Host	Radical	A_β, MHz (T, °K)	Ref
Cyclopropane	$CH_2\dot{C}HCH_2$	39.04–41.56 (153)	*a*
	$c\text{-}C_3H_6\cdot$	65.64 (153)	*a*
	$CH_3CH_2\dot{C}H_2$	93.05 (153)	*a*
1,1-Cyclopropanedicarboxylic acid	$CH_2\underset{\cdot}{C}(COOH)CH_2$		
		40–43 (298)	*b*
	$c\text{-}C_3H_4\cdot COOH$[c]	66–69 (298)	*b*
	$CH_3CH_2\dot{C}(COOH)_2$	27–31 (298)	*b*
Cyclobutane	$c\text{-}C_4H_7\cdot$	102.74 (193)	*a*
1,1-Cyclobutanedicarboxylic acid, $c\text{-}C_4H_6(COOH(D))_2$	$c\text{-}C_4H_6\cdot COOH(D)$	88–91 (77, 298)	*b*
		104–111 (4.2) ax	
		57–70 (4.2) eq	
	$CH_3CH_2CH_2\dot{C}(COOH)(D))_2$[d]	52–56 (77, 298)	*b*
		25–31 (77, 298)	
Cyclopentane	$c\text{-}C_6H_9\cdot$	98.54 (193)	*a*
1,1-Cyclopentanedicarboxylic acid, $c\text{-}C_5H_8(COOH(D))_2$	$c\text{-}C_5H_8\cdot COOH(D)$	89–93 (298)	*b*
		116–121 (4.2, 77) ax	
		58–63 (4.2, 77) eq	

[a] R. W. Fessenden and R. H. Schuler, *J. Chem. Phys.*, **39**, 2147 (1963). [b] This work; L. R. Dalton, Thesis, Harvard University, 1971. [c] This radical is unstable at ambient temperatures. [d] The concentration of this radical can be reduced below detection capabilities by thermally aging the irradiated sample at 60–70° for a few hours.

to the corresponding proton in the parent molecule. (The latter C_α–$H_{(\beta,\gamma)}$ directions were determined from the model giving the best fit of the proton ednmr data.) From this comparison it appears that the ring of the radical is not significantly rotated from that of the host molecules, indicating that sp^3 hybridization is probably retained in the radical. Further evidence for the retention of sp^3 hybridization is shown in Table IV. The β hyperfine interactions in the cyclopropyl-1-carboxylic acid and cyclopropyl radicals are nearly identical, apparently indicating that the carboxylic acid group has little effect on the beta hyperfine interaction. It is most reasonable to assume that sp^2 hybridization exists for these radicals. On the other hand quite different hyperfine interactions are observed for the hydrocarbon and monosubstituted four- and five-membered ring radicals. A possible explanation of this behavior certainly is the retention of sp^3 hybridization in the substituted radicals.

Correlation with Other Ednmr and Endor Studies. Certain comments on preliminary studies on the 1,1-cyclopentanedicarboxylic acid system are appropriate in that they correlate well with observations on the 1,1-CBDA system. The ring puckering in the five-membered ring diacid and radical appears to be describable in terms of asymmetrical barriers approximately one order of magnitude greater than the height of the barriers observed in the four-membered ring system (at 77°K the frequency of inversion is slow relative to magnetic interactions while the converse is true at ambient temperatures). The extent of puckering appears to be similar but further measurements are necessary to define the precise nature of the puckering.

Correlation with X-Ray Crystallographic Studies. The X-ray crystallographic determination of Soltzberg and Margulis[32] revealed considerable blurring of the electron density map for the H–C_γ–H methylenic group. This result is consistent with the two following possibilities: (1) the ring exists in two statically puckered conformations; (2) the ring is rapidly inverting between the above two puckered conformations.

The present ednmr studies support the latter possibility and imply a barrier to ring inversion of approximately 20 cm^{-1}. As discussed in the preceding paragraphs, dynamic puckering also appears to be involved for the radical and for the five-membered ring system.

The conformations of the four molecules per unit cell determined by ednmr and X-ray crystallography are in general in good agreement. The directions of propagation of the carboxylic acid bridge planes determined by the two techniques agree to within 5°. The existence of $P2_1/c$ symmetry is established by both techniques and the ednmr data support the contention of planar carboxylic acid bridge planes.[38] Both techniques indicate that the O4′···H8 hydrogen bond is 0.02 to 0.03 Å longer than the O2′···H7 hydrogen bond.

The conformations of the hydrocarbon ring determined from ednmr and X-ray data are in good agreement; however, because of the blurring of the electron density profile at ambient temperature and because of the difficulty of locating proton positions associated with the X-ray method, the model derived from ednmr data provides a more realistic description of the ring conformation. Unfortunately even the present ednmr data do not provide sufficient information to determine the extent of methylene rocking present. It is of considerable theoretical interest[39] to ascertain both the extent of ring puckering and methylene rocking and to relate these to the height of the barrier to ring inversion. We are currently attempting to obtain a more refined picture of ring puckering in 1,1-CBDA by investigating the selectively deuterated analogs

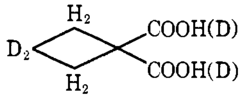

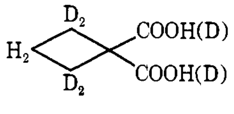

and performing variable-temperature studies. These studies should permit a uniquely detailed determination of the conformation and barrier to inversion in 1,1-CBDA crystals.

The adaptability of ednmr to determination of structures at low and variable temperatures provides a dis-

---

(38) It is not possible from the ednmr measurements to determine that the carboxylic acid bridge structures are truly planar but only that the –C(=O)OH halves (*e.g.*, O2–C5–O1–H7 and O2′–C5′–O1′–H7′) are coplanar.

(39) J. S. Wright and L. Salem, *Chem. Commun.*, 1370 (1969).

tinct advantage over the X-ray and neutron diffraction techniques. This is particularly the case for the investigation of materials with characteristic local motion. The sensitivity of the ednmr technique to the determination of the relative positions of light atoms such as protons makes this technique highly complementary to the X-ray crystallographic technique. (It should be noted that the molecular structure, as distinct from the crystal structure, is also partially accessible to nmr studies carried out in nematic solvents.[40])

Ednmr and Hydrogen Bonding. The present studies and investigation of malonic acid by Kwiram and McCalley[18,22] indicate that the empirical equation of Soda and Chiba[41]

$$\frac{e^2Qq}{h} = 310.0 - \frac{571.8}{[R(\mathrm{O}\cdots\mathrm{H})]^3}\ \mathrm{kHz}$$

where $R(\mathrm{O}\cdots\mathrm{H})$ is given in ångström units, should be modified for application to hydrogen-bonded carboxylic acid bridge structures. A more appropriate relationship between the quadrupole coupling constants and the length of the hydrogen bond appears to be

$$\frac{e^2Qq}{h} = 290 - \frac{562}{[R(\mathrm{O}\cdots\mathrm{H})]^3}\ \mathrm{kHz}$$

although we emphasize that further studies are necessary to refine the coefficients.

Comparison of the ednmr data for 1,1-CBDA with that for malonic acid[18,22] indicates that somewhat stronger hydrogen bonding exists in 1,1-CBDA. This difference in hydrogen bond strengths is also reflected in the melting points: 157° (1,1-CBDA) and 135.6° (malonic acid).

Acknowledgments. The authors express their appreciation to Dr. R. C. McCalley for many stimulating and informative discussions.

---

[40] See, for example, the results for cyclobutane reported by S. Meiboom and L. C. Snyder, *J. Chem. Phys.*, **52**, 3857 (1970).

[41] G. Soda and T. Chiba, *ibid.*, 50, 439 (1969).

Phenalenyl Dimer Cation and Its Electron Paramagnetic Resonance Spectrum[1a]

D. H. Paskovich[1b] and A. H. Reddoch*

Contribution from the Division of Chemistry, National Research Council of Canada, Ottawa K1A 0R6. *Received January 31, 1972*

Abstract: A new type of dimer cation, formed from a neutral radical and its diamagnetic cation, is reported here. The phenalenyl dimer cation $(C_{13}H_9)_2^+$ is formed on dissolving phenalene in $CF_3COCF_3 \cdot nH_2O$, $n = 2$–5. Its epr spectrum is described by the coupling constants a_1 (12 H) = 3.108 and a_2 (6 H) = 0.920 G and a g value of 2.002721.

The epr spectrum of the neutral phenalenyl radical was first reported by Calvin, *et al.*,[2] who found it in a CCl_4 solution containing phenalene which had been exposed to air. This radical can be formed in a wide range of organic solvents by dissolving phenalene,[3] which reacts with atmospheric oxygen presumably forming a hydroperoxide, which on decomposition leads to the radical. When the solution is degassed, a well-resolved epr spectrum is obtained. The coupling constants and g value are slightly solvent dependent, but typical values are $a_1 = 6.31$ G, $a_2 = 1.81$ G, and $g = 2.00260$.[3-6]

A different spectrum is obtained when a range of hexafluoroacetone (HFA) hydrates, $CF_3COCF_3 \cdot nH_2O$, $n = 2$–5, is used as a solvent. This spectrum consists of 13 septets. For $n = 4.2$ the coupling constants are a_1 (12 H) = 3.108 ± 0.002 G, a_2 (6 H) = 0.920 ± 0.002 G, and the g value is 2.002721 ± 0.000005, the latter having been corrected for second-order effects.[7] No signal was obtained with $n > 6$, and usually one was not obtained if $n \simeq 1.5$, although results were not completely reproducible in this nearly solid hydrate. When dimethoxyethane was present as well as $HFA \cdot 1.5H_2O$ only the phenalenyl signal was obtained. When D_2O was used instead of H_2O no deuteration of either phenalenyl or the new radical was detected in their spectra.

In one experiment in $HFA \cdot 2.5D_2O$ the spectra of phenalenyl and the new species were superimposed; however, the former species disappeared in a short time. Precise absolute coupling constants and g values were not obtained for this sample but good differential measurements were obtained and will be discussed below.

Since the new spectrum may be derived from that of phenalenyl by doubling the number of each type of proton and halving the coupling constants, it is clearly a dimeric species. Since the spectra are quite sharp, (the dimer line width is 88 mG compared with 80 mG for monomer in the same sample) there can be only one unpaired electron, pointing to a dimeric ion. The chemistry indicates that this must be the dimer cation $(C_{13}H_9)_2^+$. Thus the anion would be unlikely to form

---

[1] (a) Issued as NRCC No. 12688. (b) National Research Council of Canada Visiting Scientist 1967–1968.

[2] P. B. Sogo, M. Nakazaki, and M. Calvin, *J. Chem. Phys.*, 26, 1343 (1957).

[3] A. H. Reddoch, D. H. Paskovich, and A. E. Goggins, to be submitted for publication.

[4] J. E. Bennett, *Proc. Chem. Soc.*, 144 (1961).

[5] B. G. Segal, M. Kaplan, and G. K. Fraenkel, *J. Chem. Phys.*, 43, 4191 (1965).

[6] A. H. Reddoch, C. L. Dodson, and D. H. Paskovich, *ibid.*, 52, 2318 (1970).

[7] R. W. Fessenden, *ibid.*, 37, 747 (1962).